4-6-2009

Controlled Assembly of Rodlike Viruses with Polymers

Tao Li
University of South Carolina - Columbia

Laying Wu
University of South Carolina - Columbia

Nisaraporn Suthiwangcharoen
University of South Carolina - Columbia

Michael A. Bruckman
University of South Carolina - Columbia

Dayton Cash
Clemson University

See next page for additional authors

Publication Info

Published in *Chemical Communications*, Volume 2009, Issue 20, 2009, pages 2869-2871.

Controlled assembly of rodlike viruses with polymers

Tao Li,[a] Laying Wu,[a] Nisaraporn Suthiwangcharoen,[a] Michael A. Bruckman,[a] Dayton Cash,[b] JoAn S. Hudson,[b] Soumitra Ghoshroy[c] and Qian Wang*[a]

Received (in Austin, TX, USA) 30th January 2009, Accepted 12th March 2009
First published as an Advance Article on the web 6th April 2009
DOI: 10.1039/b901995b

A practical method to assemble rodlike tobacco mosaic virus and bateriophage M13 with polymers was developed, which afforded a 3D core–shell composite with morphological control.

One-dimensional (1D) nanomaterials have shown great potential in the application of optical and electronic devices, sensing and imaging, diagnostics, and drug and gene delivery,[1] due to their anisotropic structural features and their specific shape-dependant properties, such as absorptivity, photoluminescence, and conductivity.[2] Many synthetic strategies have been developed to fabricate 1D metallic, semi-conductive, polymeric and biological nanostructures. Nevertheless, effective methods to assemble nanorods into organized multi-dimensional structures are limited in scope.[3–5] Functionalization of the end part of 1D particles can lead to end-to-end, side-by-side, or even star-like structures.[3] This has been explored to develop hierarchical structures from 1D nanorods using external forces such as electric, magnetic fields, and interfacial forces.[4] Anchoring polymers on nanorods can also help in creating "amphiphilic polymer"-like nanorods to help to assemble 3D structures.[5] In this paper, we will describe a facile way to construct 3D core–shell structures using rodlike viruses and poly(4-vinylpyridine) (P4VP), a polymer showing great potential in self-assembly with other polymers or nanoparticles,[6] as building blocks.

Two viruses, tobacco mosaic virus (TMV) and bacteriophage M13, were applied in the study. TMV, with a diameter of 18 nm and length of 300 nm, is one of the most well-known rodlike viruses[7] that have been broadly used in material developments. The surface properties of TMV can be readily controlled *via* bioconjugation and genetic modification.[8] Non-covalent interactions can promote the polymerization of aniline exclusively on the surface of TMV to form conductive nanowires.[9] TMV-based biocomposite materials have also shown potential applications in the fields of nanoelectronics and energy harvesting devices.[10,11]

In a typical experiment, a solution of P4VP (Mw 60 000 Da) in dimethylformamide (DMF) was mixed with an aqueous solution of TMV at room temperature. Then, a thorough dialysis against pure water turned the solution into a faint blue and led to the formation of opalescent colloids, denoted as TMV/P4VP. Transmission electron microscopy (TEM) and field emission scanning electron microscopy (FESEM) were used to characterize the morphology of TMV/P4VP particles. Spherical core–shell structures with TMV particles coated on the P4VP ball were observed by FESEM (Fig. 1), similarly to what was found using icosahedral viral particles as building blocks.[12] The curvature of TMV/P4VP played an important role in the deformation of TMV particles. For smaller TMV/P4VP particles with diameters around 400 nm (Fig. 1(b)), TMV slightly bended itself along the curvature of the spherical structure to cover the P4VP. Although the distortion of TMV could lead to an increase in strain energy, the interfacial energy between water and hydrophobic P4VP (at neutral condition) would be greatly reduced using TMV particles to fully cover the P4VP. This process is similar to the formation of the Pickering emulsion using viral particles to stabilize oil droplets in water.[13] As the sizes of colloids became progressively larger than 500 nm (Fig. 1(c) and (d)), the TMV at the surface appeared to be much less distorted due to the lower curvature of the P4VP core.

In order to further understand the assembly process, TEM and FESEM were used to analyze the reaction mixtures at different stages. As shown in Fig. 2, TMV/P4VP pre-mixture, TMV/P4VP intermediate, and TMV/P4VP were denoted for the particles before dialysis, immediately after dialysis, and equilibrating over a long period of time after dialysis, respectively. As shown in Fig. 2(a) and (b), the morphology of TMV/P4VP pre-mixture was spherical. After a 48 h dialysis,

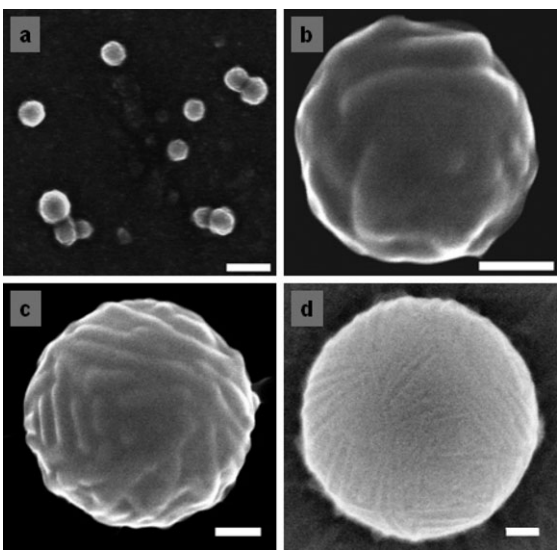

Fig. 1 Representative FESEM images of TMV/P4VP in pure water at (a) low magnification and (b–d) high magnification. The mass ratio m_{TMV}/m_{P4VP} is 0.2. Scale bars are 1 μm in (a) and 100 nm in (b–d).

[a] *Department of Chemistry and Biochemistry and Nanocenter, University of South Carolina, 631 Sumter Street, Columbia, SC 29208, USA. E-mail: wang@mail.chem.sc.edu*
[b] *Clemson University Electron Microscope Facility, Clemson Research Park, Anderson, SC 29625, USA*
[c] *Electron Microscopy Center of University of South Carolina, 715 Sumter Street, Columbia, SC 29625, USA*

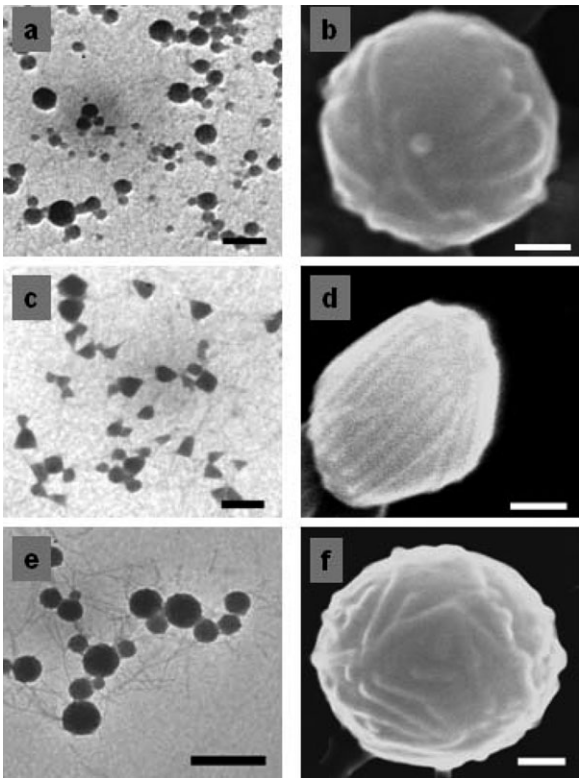

Fig. 2 Representative TEM and FESEM images of TMV/P4VP before dialysis (a, b), immediately after dialysis (c, d), and final TMV/P4VP particles (e, f) (the mass ratio m_{TMV}/m_{P4VP} is 0.2). Scale bars are 500 nm in (a, c, e) and 100 nm in (b, d, f).

the morphology of TMV/P4VP intermediate changed to irregular shapes as shown in Fig. 2(c). FESEM (Fig. 2(d)) clearly shows the rhomboidal colloids with TMVs coated on the surface. After a further equilibrating for 120 h, the colloids were transformed into final product, TMV/P4VP, with spherical shapes, as shown in Fig. 2(e) and (f). Fig. 2(f) shows a single TMV/P4VP particle that is thoroughly covered with TMV on the surface. Comparing with TMV/P4VP pre-mixture (Fig. 2(b)), the final particle had much better coverage of TMV on surface.

Based on above observations, we propose a three-step assembly mechanism to outline the process (Scheme 1). In step **A**, P4VP in a small quantity of DMF is mixed with TMV in water and forms a TMV/P4VP pre-mixture. Since P4VP cannot be dissolved in water, it forms aggregates covered by TMV particles. The existence of DMF can still solvate the P4VP, therefore, fewer TMV particles are needed to cover the aggregates, which are of spherical morphology to reduce the interfacial energy. Upon dialysis during step **B**, as the amount of DMF decreases, the solubility of P4VP decreases, thereby causing the phase separation of P4VP. Hence more TMV particles moved to the surface of the phase-separated P4VP to reduce the interfacial energy between the polymer and water. During this process, TMV particles prefer to maintain the rod-like structure and could not be bent more than its modulus allowed, which leads to the irregular shapes of the TMV/P4VP intermediate. However, after a long time of equilibration in step **C**, TMV particles slowly distort to adapt

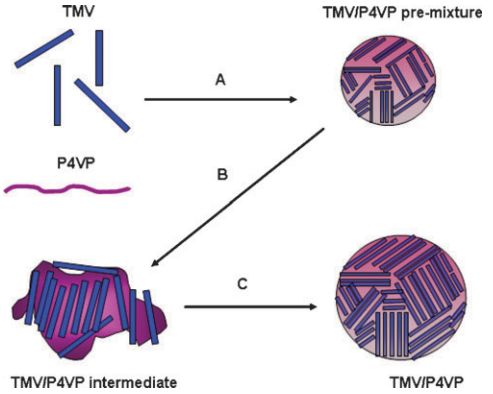

Scheme 1 Illustration of the assembly process of TMV and P4VP. Step **A**, mixing of TMV and P4VP in DMF (3%) and water to give TMV/P4VP pre-mixture. Step **B**, dialysis against water for 48 h affording TMV/P4VP intermediate. Step **C**, equilibrating at room temperature for 120 h to form TMV/P4VP.

the curvature of a spherical shape and transform to the final TMV/P4VP.

To further confirm the EM results, laser confocal microscopy (LCM) was also used to examine the coverage of TMV. Fluorescently modified TMV was prepared using Cu(I)-catalyzed azide–alkyne 1,3-dipolar cycloaddition (CuAAC) reaction with anthracene-azide as reported.[8b] Using anthracene modified TMV, the final TMV/P4VP showed bright fluorescence observed under LCM (Fig. 3(a)). Another concern was whether TMVs were only located on the surface of TMV/P4VP, which cannot be answered by either optical microscopic analyses or normal EM analyses. Therefore, a TEM cross section method was employed. TEM tomography was developed to identify the assembly between the protein cage and P4VP.[14] Double staining caused the virus components to become electron-dense groups compared to the surroundings, and showed a ring-like structure (Fig. 3(b)), indicating that TMVs were only located on the surfaces of P4VP balls.

Another rodlike biological particle, bacteriophage M13, a well-known biological building block for materials science,[15] was also used in our study. M13 is about 6.5 nm in diameter and 880 nm in length, and consists of 2700 major coat proteins helically stacked around its single-stranded DNA. When M13 was co-assembled with P4VP in solution following a similar protocol as TMV, M13/P4VP composites formed as spherical

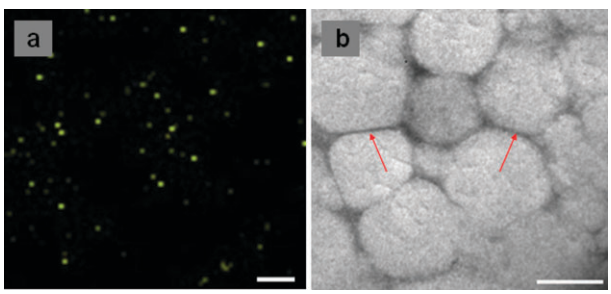

Fig. 3 Laser confocal microscopy image (a) and TEM cross section image (b) of TMV/P4VP structures. Anthracene modified TMV was used in the study. In (b), red arrows showed the edges of dark rings, which are viral particles after double staining. The mass ratio m_{TMV}/m_{P4VP} is 0.2. Scale bars are 4 μm in (a) and 500 nm in (b).

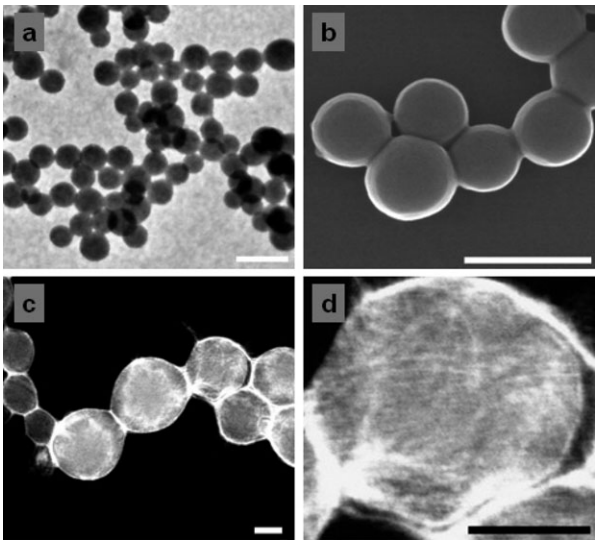

Fig. 4 Representative TEM (a) and FESEM (b) images of M13/P4VP. (c) Low magnification and (d) high resolution dark field TEM images of M13/P4VP (the mass ratio m_{M13}/m_{P4VP} is 0.20). Scale bars are 200 nm in (a, b) and 50 nm in (c, d).

shapes, denoted as M13/P4VP, as shown by TEM and SEM (Fig. 4(a) and (b)). Although the length of M13 is greater than the diameter of most particles, it can twist and wrap around the P4VP assemblies due to the flexibility of M13.[16] It was difficult to detect any M13 particles using regular TEM/SEM analyses because 6.5 nm (diameter of M13) was at the limit for a biological sample for SEM measurement. In order to confirm the existence of M13 on the surface of P4VP, dark field high resolution TEM was conducted. As shown in Fig. 4(c) and (d), it can be clearly observed that P4VP particles were covered with M13 viruses.

In summary, a facile method to construct 3D structures using the rodlike biological particles TMV and M13 has been developed. During the self-assembly process of TMV/P4VP, morphological transformation and TMV deformation were observed. The results confirmed that TMVs serve as a "surfactant" to stabilize the P4VP particles in water by covering their exterior surface. This unique self-assembly behavior will open up a new way to assemble and organize rodlike particles hierarchically.

We are grateful for financial support from US NSF, the Alfred P. Sloan Foundation, the Camille Dreyfus Teacher-Scholarship, the US DoD, and the W. M. Keck Foundation. We are also thankful for the Gagandeep Kaur for her help with confocal microscopy imaging.

Notes and references

1 (*a*) C. J. Murphy, T. K. Sau, A. Gole, C. J. Orendorff, J. Gao, L. Gou, S. Hunyadi and T. Li, *J. Phys. Chem. B*, 2005, **109**, 13857; (*b*) Y. Xia, P. Yang, Y. Sun, Y. Wu, B. Mayers, B. Gates, Y. Yin, F. Kim and H. Yan, *Adv. Mater.*, 1999, **15**, 353.

2 (*a*) X. Duan, Y. Huang, R. Agarwal and C. M. Lieber, *Nature*, 2003, **421**, 241; (*b*) T. Rueckes, K. Kim, E. Joselevich, G. Y. Tseng, C. Cheung and C. M. Lieber, *Science*, 2000, **289**, 94.

3 (*a*) K. K. Caswell, J. N. Wilson, U. H. F. Bunz and C. J. Murphy, *J. Am. Chem. Soc.*, 2003, **125**, 13914; (*b*) P. K. Sudeep, S. T. Joseph and K. G. Thomas, *J. Am. Chem. Soc.*, 2005, **127**, 6516.

4 (*a*) J. C. Love, A. R. Urbach, M. G. Prentiss and G. M. Whitesides, *J. Am. Chem. Soc.*, 2003, **125**, 12696; (*b*) S. Gupta, Q. Zhang, T. Emrick and T. P. Russell, *Nano Lett.*, 2006, **6**, 2066.

5 (*a*) Z. H. Nie, D. Fava, E. Kumacheva, S. Zou, G. C. Walker and M. Rubinstein, *Nat. Mater.*, 2007, **6**, 609; (*b*) Z. H. Nie, D. Fava, M. Rubinstein and E. Kumacheva, *J. Am. Chem. Soc.*, 2008, **130**, 3683.

6 (*a*) D. Y. Chen and M. Jiang, *Acc. Chem. Res.*, 2005, **38**, 494; (*b*) X. K. Liu and M. Jiang, *Angew. Chem., Int. Ed.*, 2006, **45**, 3846; (*c*) L. Nie, S. Liu, W. Shen, D. Y. Chen and M. Jiang, *Angew. Chem., Int. Ed.*, 2007, **46**, 6321; (*d*) Y. W. Zhang, M. Jiang, J. X. Zhao, X. W. Ren, D. Y. Chen and G. Z. Zhang, *Adv. Funct. Mater.*, 2005, **15**, 695; (*e*) T. Li, Z. Niu, T. Emrick, T. P. Russell and Q. Wang, *Small*, 2008, **4**, 1624.

7 (*a*) M. Zaitlin, *AAB Descriptions Plants Viruses*, 2000, **370**, 8; (*b*) R. N. Perham and T. M. A. Wilson, *Virology*, 1978, **84**, 293; (*c*) L. King and R. Leberman, *Biochim. Biophys. Acta*, 1973, **322**, 279; (*d*) T. M. A. Wilson and R. N. Perham, *Virology*, 1985, **140**, 21.

8 (*a*) T. L. Schlick, Z. Ding, E. W. Kovacs and M. B. Francis, *J. Am. Chem. Soc.*, 2005, **127**, 3718; (*b*) M. A. Bruckman, G. Kaur, L. A. Lee, F. Xie, J. Sepulveda, R. Breitenkamp, X. Zhang, M. Joralemon, T. P. Russell, T. Emrick and Q. Wang, *ChemBioChem*, 2008, **9**, 519; (*c*) W. S. Tan, C. L. Lewis, N. E. Horelik, D. C. Pregibon, P. S. Doyle and H. Y, *Langmuir*, 2008, **24**, 12483; (*d*) H. Y, G. W. Rubloff and J. N. Culver, *Langmuir*, 2007, **23**, 2663.

9 (*a*) Z. Niu, M. A. Bruckman, V. S. Kotakadi, J. He, T. Emrick, T. P. Russell, L. Yang and Q. Wang, *Chem. Commun.*, 2006, 3019; (*b*) Z. Niu, J. Liu, L. A. Lee, M. A. Bruckman, D. Zhao, G. Koley and Q. Wang, *Nano Lett.*, 2007, **7**, 3729; (*c*) Z. Niu, M. Bruckman, S. Li, L. A. Lee, B. Lee, S. V. Pingali, P. Thiyagarajan and Q. Wang, *Langmuir*, 2007, **23**, 6719.

10 (*a*) R. J. Tseng, C. Tsai, L. Ma, J. Oyang, C. S. Ozkan and Y. Yang, *Nat. Nanotechnol.*, 2006, **1**, 72; (*b*) S. V. Kalinin, S. Jesse, W. L. Liu and A. A. Balandin, *Appl. Phys. Lett.*, 2006, **88**, 153902; (*c*) R. A. Miller, A. D. Presley and M. B. Francis, *J. Am. Chem. Soc.*, 2007, **129**, 3104.

11 (*a*) H. Yi, G. W. Rubloff and J. N. Culver, *Langmuir*, 2007, **23**, 2663; (*b*) H. Yi, S. Nisar, S. Y. Lee, M. A. Powers, W. E. Bentley, G. F. Payne, R. Ghodssi, G. W. Rubloff, M. T. Harris and J. N. Culver, *Nano Lett.*, 2005, **5**, 1931; (*c*) S. Balci, K. Noda, A. M. Bittner, A. Kadri, C. Wege, H. Jeske and K. Kern, *Angew. Chem., Int. Ed.*, 2007, **46**, 3149; (*d*) M. Knez, M. Sumser, A. M. Bittner, C. Wege, H. Jeske, T. P. Martin and K. Kern, *Adv. Funct. Mater.*, 2004, **14**, 116; (*e*) V. A. Fonoberov and A. A. Balandin, *Nano Lett.*, 2005, **5**, 1920.

12 T. Li, B. Ye, Z. Niu, P. Thompson, S. Seifert, B. Lee and Q. Wang, *Chem. Mater.*, 2009, **21**, 1046.

13 J. T. Russell, Y. Lin, A. Böker, S. Long, P. Carl, H. Zettl, J. He, K. Sill, R. Tangirala, T. Emrick, K. Littrell, P. Thiyagarajan, D. Cookson, A. Fery, Q. Wang and T. P. Russell, *Angew. Chem., Int. Ed.*, 2005, **44**, 2420.

14 Under the optimal cross section condition, the sample was pelleted under 13000 rpm and then fixed with 0.1 M cacodalate buffered 2.5% glutaraldehyde for 3 h. Afterwards, the specimen was infiltrated in acetone/resin. With a good infiltration, the sample was embedded into Spurr resin at 60 °C for 24 h. Under light microscope, the embedded sample was trimmed and microtomed to 60–100 nm thickness, and then mounted onto grids. After a double staining with uranyl acetate and lead nitrate, the sample was analyzed by TEM.

15 (*a*) S. W. Lee, C. Mao, C. E. Flynn and A. M. Belcher, *Science*, 2002, **296**, 892; (*b*) K. T. Nam, D. W. Kim, P. J. Yoo, C. Y. Chiang, N. Meethong, P. T. Hammond, Y. M. Chiang and A. M. Belcher, *Science*, 2006, **312**, 885.

16 K. T. Nam, B. R. Peelle, S. W. Lee and A. M. Belcher, *Nano Lett.*, 2004, **4**, 23.